Available online at www.sciencedirect.com
SCIENCE DIRECT®
Cardiovascular Research 60 (2003) 557–568
Cardiovascular Research
www.elsevier.com/locate/cardiores

Induction of myocardial biglycan in heart failure in rats—an extracellular matrix component targeted by AT_1 receptor antagonism

Mohammed Shakil Ahmed[a,b], Erik Øie[a,b], Leif Erik Vinge[a,b], Arne Yndestad[c], Geir Øystein Andersen[a,d], Yvonne Andersson[a,b], Toril Attramadal[a,b], Håvard Attramadal[a,b,*]

[a] *MSD Cardiovascular Research Centre, Rikshospitalet University Hospital, University of Oslo, Oslo, Norway*
[b] *Institute for Surgical Research, Rikshospitalet University Hospital, University of Oslo, Oslo, Norway*
[c] *Research Institute for Internal Medicine, Rikshospitalet University Hospital, University of Oslo, Oslo, Norway*
[d] *Department of Pharmacology, Rikshospitalet University Hospital, University of Oslo, Oslo, Norway*

Received 13 December 2002; accepted 29 August 2003

Time for primary review 21 days

Abstract

Objective: Cardiac remodelling associated with congestive heart failure typically involves dilatation of the ventricular cavities, cardiomyocyte hypertrophy and alterations of extracellular matrix. Biglycan is an extracellular proteoglycan with several recently appreciated functions including cell adhesion, collagen fibril assembly, and growth factor interactions. The aims of this study were to investigate the regulation of biglycan expression and to elucidate the site(s) of synthesis of biglycan in myocardial tissue in an experimental model of heart failure (HF). **Methods:** Myocardial tissue samples were obtained from rats with myocardial infarction (MI) subsequent to ligation of the left coronary artery. Northern blot analysis and real-time quantitative RT-PCR were employed to investigate mRNA levels. The cellular distribution of biglycan was analysed by in situ hybridisation and immunohistochemistry. **Results:** Myocardial biglycan mRNA levels in non-ischemic tissue of both left and right ventricles of heart failure rats were substantially elevated as compared to sham-operated rats. Although expression levels peaked 7 days after MI (13-fold increase compared to the sham group, $P < 0.05$), substantial elevations of biglycan mRNA were observed throughout the study period. Analysis of cellular distribution revealed that biglycan expression was confined to myocardial fibroblasts and vascular endothelial cells. In cardiac fibroblasts isolated from failing hearts, biglycan mRNA levels were markedly elevated compared with fibroblasts from sham-operated rats. In addition, in rats with ischemic heart failure treatment with the AT_1 receptor antagonist losartan (12.5 $mg \cdot kg^{-1}$ b.i.d. per os, for 25 days) prevented the increase of myocardial biglycan as well as TGF-β_1 mRNA. **Conclusion:** This report demonstrates global induction of myocardial biglycan mRNA in heart failure. Myocardial biglycan expression could be targeted by AT_1 receptor antagonism, an intervention well documented to halt cardiac remodelling in heart failure. Furthermore, the study provides evidence that angiotensin II is a regulator of biglycan expression in cardiac fibroblasts.

Keywords: Heart failure; Remodelling; Gene expression; Extracellular matrix; Angiotensin

1. Introduction

Congestive heart failure is associated with structural alterations of the heart collectively referred to as cardiac remodelling. Cardiac remodelling has both macroscopic and microscopic correlates. Typically, dilatation of the ventricular cavities, cardiomyocyte hypertrophy, and alter-

* Corresponding author. Institute for Surgical Research, A3.1013, Rikshospitalet University Hospital, N-0027 Oslo, Norway. Tel.: +47-23-073520; fax: +47-23-073530.
E-mail address: havard.attramadal@klinmed.uio.no (H. Attramadal).

0008-6363/$ - see front matter © 2003 European Society of Cardiology. Published by Elsevier B.V. All rights reserved.
doi:10.1016/j.cardiores.2003.08.017

ations of the composition and the amount of extracellular matrix (ECM) can be observed [1]. Although these responses are initially beneficial, sustained alterations impair left ventricular function and act as strong predictors of mortality in heart failure patients. However, the underlying molecular mechanisms of myocardial remodelling are still poorly understood.

We have used the differential gene display technique to identify genes that are regulated in myocardial tissue during post-infarction failure, and thus, putatively involved in the cardiac remodelling process. One of the genes that were substantially induced in the failing heart was the small leucine-rich proteoglycan, biglycan. Proteoglycans are complex macromolecules that consist of a protein core and one or more glycosaminoglycan side chains covalently bound to the core protein [2]. These molecules, which are prominent constituents of both the ECM and the cellular basal membrane, have recently become a focus of attention since they have been shown to be involved in a multitude of cellular functions. Recent evidence indicates that proteoglycans may play important roles in cell adhesion, growth factor interactions, and matrix assembly [3]. Biglycan has been reported to play roles in organisation of fibrillar collagen due to its ability to bind collagen type I [4]. In addition, biglycan may affect cell migration by modulating interactions of cell surface receptors with its matrix ligands [5] and influence cell growth by regulation of the availability and function of growth factors, for example, by binding transforming growth factor-β (TGF-β) [3,6]. These recently appreciated effects of biglycan suggest that this proteoglycan may be an important factor in the mechanisms of myocardial remodelling of the failing heart.

Biglycan has been identified in diverse cell types, including endothelial cells [7], fibroblasts [8], myofibroblasts [7,9], and vascular smooth muscle cells [9]. Furthermore, it has previously been reported that biglycan mRNA levels are increased in the infarcted zone after MI, suggesting a role during healing of the infarcted area [10]. However, no data are available regarding regulation of biglycan in noninfarcted, viable regions of the failing heart. Whereas reparative fibrosis appearing at the site of MI is essential to preserving the structural integrity of the afflicted heart, interstitial myocardial fibrosis occurring remote to the MI increases tissue stiffness leading to decreased compliance of the ventricles and diastolic ventricular dysfunction.

To elucidate the expression pattern of biglycan during post-infarction failure, we investigated the time course of biglycan mRNA expression in the non-ischemic regions of the left and the right ventricles during myocardial remodelling secondary to the induction of MI. Secondly, the cellular distribution of biglycan mRNA and protein in myocardial tissue was investigated by in situ hybridisation and immunohistochemistry, respectively. Thirdly, since angiotensin II (Ang II) has been reported to be involved in the pathophysiology of myocardial remodelling after MI, we investigated to what extent Ang II type 1 (AT_1) receptor antagonism would affect myocardial biglycan mRNA expression in post-infarction failure.

2. Methods

2.1. Animal preparation

We used the left coronary artery-ligated rat model of HF as previously described [11]. Briefly, male Wistar rats (~ 250 g) were anaesthetized with 1% isoflurane in 1/3 O_2 and 2/3 N_2O and subjected to left thoracotomy with subsequent ligation of the proximal portion of the left coronary artery. Except for ligation of the artery, sham-operated rats underwent the same procedure. The animal experiments and housing were in accordance with institutional guidelines and national legislation conforming to The European Convention for The Protection of Vertebrate Animals Used for Experimental and Other Scientific Purposes of 18 March 1986.

2.2. Study protocol

The aim of the first series of experiments was to investigate regulation and cellular distribution of myocardial biglycan mRNA and protein during development of HF after MI. HF rats ($n = 5$ in each group) and sham-operated rats ($n = 4$ in each group) were euthanised 2, 7, or 42 days after induction of MI. In rats subjected to MI, left ventricular end-diastolic pressure (LVEDP) >15 mm Hg was employed as the criteria of HF and of inclusion in the study.

The purpose of the second series of experiments was to investigate the effects of AT_1 receptor antagonism on myocardial biglycan expression after MI in rats. MI rats were randomised to treatment for 25 days with the AT_1 receptor antagonist losartan (Merck Sharp & Dohme, Whitehouse Station, USA; 12.5 $mg \cdot kg^{-1}$ b.i.d. per os; $n = 6$) or vehicle (water; $n = 5$) administered by gavage. The treatment protocol was initiated 3 days after induction of MI to minimize the possibility of a direct effect of losartan on infarct size. Sham-operated rats that received no treatment were also included in the study ($n = 5$).

2.3. Hemodynamic measurements and tissue sampling

On the day of the experiments, the rats were anaesthetized with gas anaesthesia containing 1% isoflurane in 1/3 O_2 and 2/3 N_2O. Left ventricular systolic pressure (LVSP) and LVEDP were recorded by a 2F micromanometer-tipped catheter (model SPR-407, Millar Instruments, Houston, TX, USA) inserted through the right carotid artery. After completion of the hemodynamic measurements, the rats were euthanised by excision of the heart. The right and left ventricles were sectioned separating noninfarcted myocardium from the infarcted area. Contamination of viable myocardial tissue with necrotic tissue was carefully avoided.

Rat hearts were perfused and fixed in 4% paraformaldehyde for 4 h (in situ hybridisation) or in Bouin's solution [2% paraformaldehyde and 0.2% picric acid in phosphate buffered saline (PBS)] for 5 h (immunohistochemistry).

2.4. Isolation of rat biglycan cDNA

Total RNA was prepared from rat myocardial tissues by acid-phenol/chloroform extraction in the presence of chaotropic salts (Trizol, Life Technologies, Gaithersburg, MD, USA). A 406-bp fragment of rat biglycan cDNA (nt 360–764; GenBank accession no. U17834) was amplified by RT-PCR using the biglycan-specific oligonucleotide primers 5′-TTG-GGT-CTG-AAG-ACT-GTG-CCC-3′ (upstream) and 5′-CAG-GTA-GTT-GAG-CTT-CAG-GCC-3′ (downstream) corresponding to nucleotide positions 360–380 and 744–764, respectively. The resulting RT-PCR product was subcloned into pBluescript SK^+ cloning vector (Stratagene, USA) and verified by DNA sequence analysis using the dideoxy chain termination method and used as probe for Northern blot analysis or in situ hybridisation.

2.5. Northern blot analysis

Total RNA (30 μg) from each sample was separated on agarose/formaldehyde (1.5%/6.6%) gels and transferred to nylon membranes (Hybond N, Amersham) by capillary blotting. Northern blot analysis was performed using the 406-bp biglycan cDNA fragment. The membranes were hybridised with [^{32}P]-labelled cDNA probes (specific activity $\sim 10^9$ cpm/μg) radiolabeled by random priming, washed stringently (0.1 × SSC at 60 °C; 2 × 20 min), and subsequently exposed to phosphor screens and scanned by a laser scan phosphorimager (445 SI, Molecular Dynamics, Sunnyvale, CA, USA). The autoradiographic signals were analysed by densitometry (ImageQuant, Molecular Dynamics). To control for variations in RNA loading and transfer efficiencies, the blots were rehybridised with a glyceraldehyde-3-phosphate dehydrogenase (GAPDH) cDNA probe as the housekeeping gene (fragment of rat GAPDH cDNA; nt 458–994, GenBank accession no. M17701).

2.6. Quantitative real-time RT-PCR analysis

Reverse transcription (RT) and PCR of each sample were performed in triplicates using the TaqMan PCR Core Reagent Kit and the ABI Prism 7700 Sequence Detector and software (Applied Biosystems, Foster City, CA, USA) according to the manufacturer's instructions. Sequence-specific PCR primers and TaqMan probes were designed using the Primer Express software version 1.5 (Applied Biosystems); see Table 1 for details. A standard curve for each cDNA was obtained by performing amplifications from serial dilutions of myocardial total RNA. For all specific mRNA amplified linear inverse correlations were observed between amount of RNA and C_T values (number of cycles at threshold lines). mRNA expression levels are presented relative to expression levels of the housekeeping genes GAPDH or 18S to normalize for variations in amount of RNA, purity, etc.

2.7. In situ hybridisation

The Bluescript SK^+ plasmid containing the 406-bp biglycan cDNA fragment (nt 360–764) was linearized with either *Eco*RV or *Bam*HI to synthesize digoxigenin-labeled antisense and sense ribonucleotide probes using either T7 or T3 polymerase, respectively. Paraffin-embedded (6 μm) sections of rat hearts were deparaffinised in xylene, rehydrated and treated with 0.3% Triton X-100 in PBS for 15 min. The sections were permeabilised with 10 μg/ml of proteinase K (Boehringer Mannheim, Indianapolis, IN, USA), acetylated with 0.25% acetic anhydride, and subsequently dehydrated in ethanol. Prehybridisation buffer (4 × SSC, 40% formamide, 1 × Denhardt's solution, 10% dextran, and 250 μg/ml sonicated salmon sperm DNA) was applied for at least 2 h at 42 °C. Subsequently, digoxigenin-labeled riboprobe (5 ng/μl) was added and hybridised overnight in a humidified chamber at 42 °C. After hybridisation, the sections were rinsed, treated with RNase A and finally washed in 0.1 × SSC (2 × 30 min at 60 °C). After blocking, the sections were incubated with alkaline phosphatase-conjugated Fab fragment of sheep anti-digoxigenin IgG (1:500; Boehringer Mannheim) and positive signals were detected by the NBT/BCIP colour substrate system.

2.8. Immunohistochemistry

Immunohistochemical analysis was performed as described previously [12]. Briefly, the tissue sections were incubated with anti-biglycan IgG (kindly provided by

Table 1
Oligonucleotide primers and probes used for real-time quantitative PCR analysis of biglycan and TGF-β_1 mRNA levels

Oligonucleotide	Sequence	Position
Sense (biglycan)	5′-CGGAACATGAACTGCATTGAGAT-3′	672–694
Antisense (biglycan)	5′-GTAGTTGAGCTTCAGGCCATCAA-3′	739–761
Probe (biglycan)	5′-CCTGGAGAACAGTGGCTTTGAACCCG-3′	707–732
Sense (TGF-β_1)	5′ AAGAAGTCACCCGCGTGCTA3′	729–748
Antisense (TGF-β_1)	5′ TGTGTGATGTCTTTGGTTTTGTCA3′	775–798
Probe (TGF-β_1)	5′ TGGTGGACCGCAACAAGGCAATC3′	750–772

Martin Altenburger, Department of Physiological Chemistry, University of Munster, Germany) and subsequently immunostained with the avidin–biotin–peroxidase system (Vectastain Elite kit, Vector Laboratories, USA) according to the manufacturer's instructions. Immunostaining was visualised by incubating the sections with diaminobenzidine as the chromogen in a commercial metal enhanced system (Pierce Chemical, USA). The sections were counterstained with haematoxylin.

2.9. Generation of recombinant adenovirus encoding the rat AT_{1A} receptor

Recombinant adenovirus encoding the AT_{1A} receptor (Ad-AT_{1A}) was generated using the Adeno-X Expression System (BD Biosciences Clontech, California, USA). Briefly, the open reading frame of the rat AT_{1A} receptor cDNA (GenBank accession no. NM_030985) was amplified by RT-PCR of total RNA from myocardial tissue and subcloned into the shuttle vector pShuttle (BD Biosciences Clontech). The cDNA sequence was verified by DNA sequence analysis. Adenovirus expressing the AT_{1A} receptor (Ad-AT_{1A}) was generated by transferring the pShuttle expression cassette containing the AT_{1A} receptor cDNA into circular adenoviral genome by in vitro ligation. Recombinant adenovirus was obtained by transfection of adenoviral DNA into HEK 293 cells. Recombinant adenovirus was purified by ion exchange chromatography (Virapur, USA) and infectious titer was determined using the Adeno-X Rapid Titer Kit (BD Biosciences Clontech). Expression of receptor activity was analysed by radioligand binding analysis as previously described [13]. An adenovirus carrying the *E. coli* β-galactosidase gene (Ad-LacZ) was constructed in the same manner and used as a negative control in all experiments.

2.10. Isolation of cardiac fibroblasts and adenovirus infection in vitro

Rat cardiac fibroblasts were obtained from hearts of HF rats and sham-operated rats by differential centrifugation of cardiac cells released after reverse Langendorf perfusion and enzymatic digestion of the hearts as described previously [14]. The homogeneity of these primary isolates was assessed by immunocytochemistry using anti-vimentin immunoreactivity (anti-porcine vimentin IgG_1-kappa, clone V9, Zymed Laboratories, California, USA) as fibroblast marker and anti-rat von Willebrand factor immunoreactivity (purified polyclonal anti-rat von Willebrand factor, Cedarlane, Ontario, Canada), as endothelial cell marker. The non-myocyte cell fraction contained more than 90% vimentin-positive fibroblasts. The cells from sham-operated rats were plated onto noncoated cell culture dishes, maintained and propagated in Dulbecco's modified Eagle's medium (DMEM; Life Technologies, Gaithersburg, MD) supplemented with 10% fetal calf serum (FCS; Bio-Whittaker) and 40 μg/ml garamycin in a humidified atmosphere containing 5% CO_2 at 37 °C. After the first passage, >95% of the cells stained positive for vimentin and <1% displayed immunoreactivity against von Willebrand factor.

For adenoviral infection, cells were seeded at a density of 5×10^5/60-mm plate. The monolayers were infected with virus in DMEM containing 2% FCS at a multiplicity of infection (MOI) of 100. After 4 h, the medium containing virus was removed and DMEM containing 2% FCS was added. The cells were analysed 48 h after infection.

2.11. Statistical analysis

All values are expressed as mean ± S.E.M. Statistical analysis was assessed by the Mann–Whitney test. P values < 0.05 were considered to be statistically significant.

3. Results

3.1. Hemodynamic measurements

Hemodynamic measurements recorded after ligation of the left coronary artery revealed substantial and progressive LV dysfunction in the HF rats. As shown in Table 2, LVSP was significantly lower and LVEDP significantly higher in the HF rats as compared to the sham-operated rats at all time points.

3.2. Myocardial expression of biglycan mRNA during HF

Induction of biglycan mRNA was determined by analysis of the time course of myocardial biglycan mRNA levels after MI. Total RNA was isolated from the left and right ventricles of sham-operated control ($n=4$) and MI ($n=5$) rats at 2, 7, and 42 days after MI, and the RNA expression levels were determined by Northern blot analysis. The time course of biglycan mRNA expression in the non-ischemic region of the left and in the right ventricles is illustrated in Figs. 1 and 2, respectively. Biglycan mRNA levels were low, but consistently detectable in both ventricles of sham-operated rats. After induction of MI, a marked and significant increase of biglycan mRNA levels

Table 2
Hemodynamic measurements after induction of MI or sham operation

	LVSP, mm Hg	LVEDP, mm Hg
Sham ($n=4$)	118 ± 3	4 ± 1
HF 2 days post-MI ($n=5$)	99 ± 5*	22 ± 1*
HF 7 days post-MI ($n=5$)	105 ± 4*	25 ± 2*
HF 42 days post-MI ($n=5$)	96 ± 4*	26 ± 3*

LVSP, LV systolic pressure; LVEDP, LV end-diastolic pressure.
Values are mean ± S.E.M.
* $P<0.05$ vs. sham.

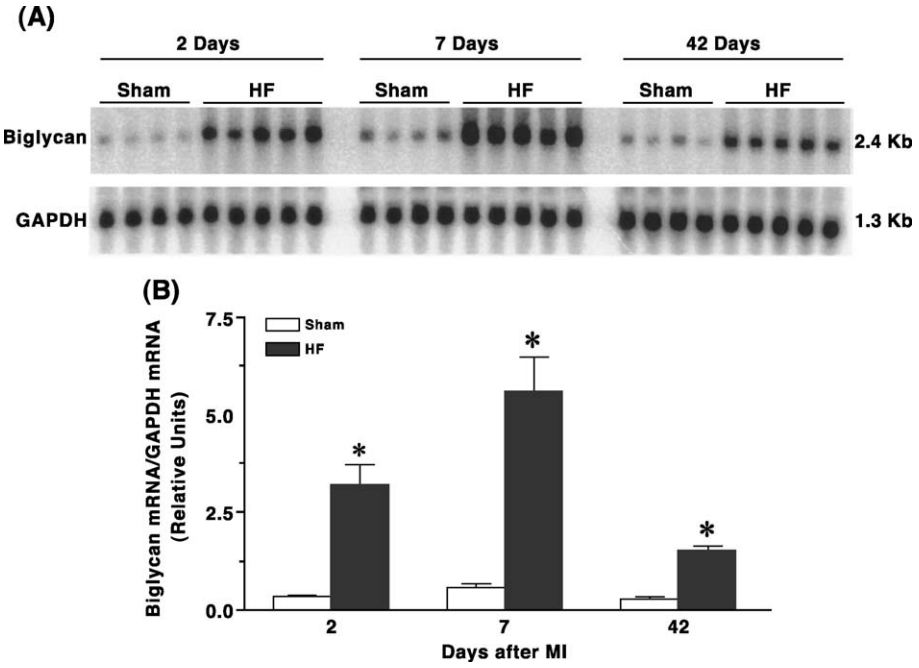

Fig. 1. Northern blot analysis of myocardial biglycan and GAPDH mRNA levels in the left ventricles of HF rats at 2, 7, and 42 days after induction of MI and corresponding sham-operated rats. Analysis was performed as detailed in Methods. Autoradiograph of Northern blot (A). Histogram demonstrating results of densitometric analysis of the autoradiograph (B). The bars represent biglycan mRNA levels relative to GAPDH mRNA levels for sham-operated rats (open bars) and HF rats (closed bars). Values are mean ± S.E. of each group for sham-operated and HF rats ($n = 4$ sham-operated rats, $n = 5$ HF rats). * $P < 0.05$ vs. sham-operated rats. Data are representative of three independent experiments.

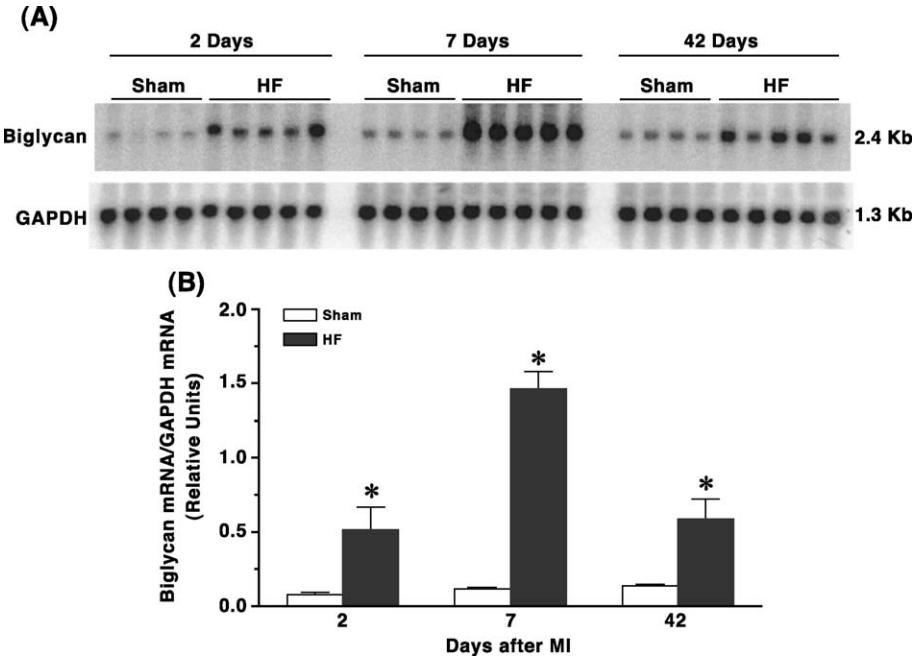

Fig. 2. Northern blot analysis of myocardial biglycan and GAPDH mRNA levels in the right ventricles of HF rats at 2, 7, and 42 days after induction of MI and corresponding sham-operated rats. Analysis was performed as detailed in Methods. Autoradiograph of Northern blot (A). Histogram demonstrating results of densitometric analysis of the autoradiograph (B). The bars represent biglycan mRNA levels relative to GAPDH mRNA levels for sham-operated rats (open bars) and HF rats (closed bars). Values are mean ± S.E. of each group for sham-operated and HF rats ($n = 4$ sham-operated rats, $n = 5$ HF rats). * $P < 0.05$ vs. sham-operated rats. Data are representative of three independent experiments.

was observed in both ventricles of HF rats as compared to the corresponding sham-operated rats throughout the study period. Already 2 days after MI, 9- and 7-fold elevations of biglycan mRNA levels were seen in the left and the right ventricles, respectively, as compared to the sham group ($P < 0.05$). Seven days after induction of MI, myocardial biglycan mRNA levels in the left and the right ventricles were 9- and 13-fold, respectively, above the

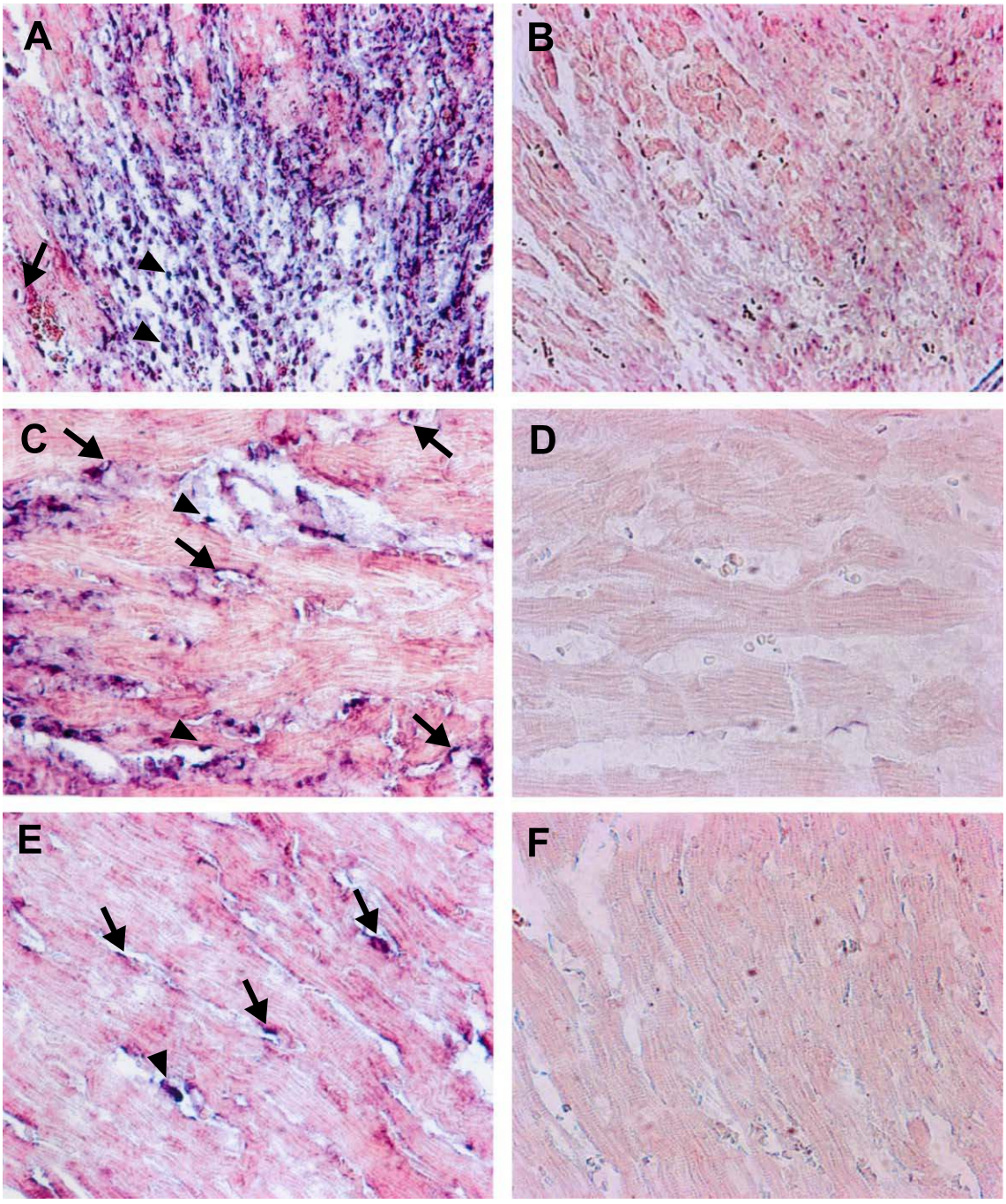

Fig. 3. Photomicrographs demonstrating in situ hybridisation of biglycan mRNA in failing rat heart. The myocardial tissue sections showing a strong antisense riboprobe staining of biglycan mRNA in the granulation tissue and fibrotic tissue radiating from the ischemic region into the viable myocardium (A). Section from fibrotic tissue radiating from the ischemic region into the viable myocardium depicting signals of biglycan mRNA in fibroblast-like cells (arrowheads) and vascular endothelial cells (arrows) (C). Tissue section from the non-ischemic LV remote from the infarcted region demonstrating antisense riboprobe staining of biglycan mRNA in fibroblast-like cells and vascular endothelial cells (E). Control sections from the corresponding areas hybridised with the sense riboprobe did not reveal any positive signals (B, D, F). Magnification × 400.

levels in the sham-operated groups ($P<0.05$). Although the myocardial biglycan mRNA expression profile demonstrated a biphasic course with a decline at 42 days after MI compared to the levels observed at 7 days, biglycan mRNA levels in both the left and the right ventricles were still substantially elevated 42 days after MI compared to the sham-operated group (5- and 4-fold increase, respectively, $P<0.05$).

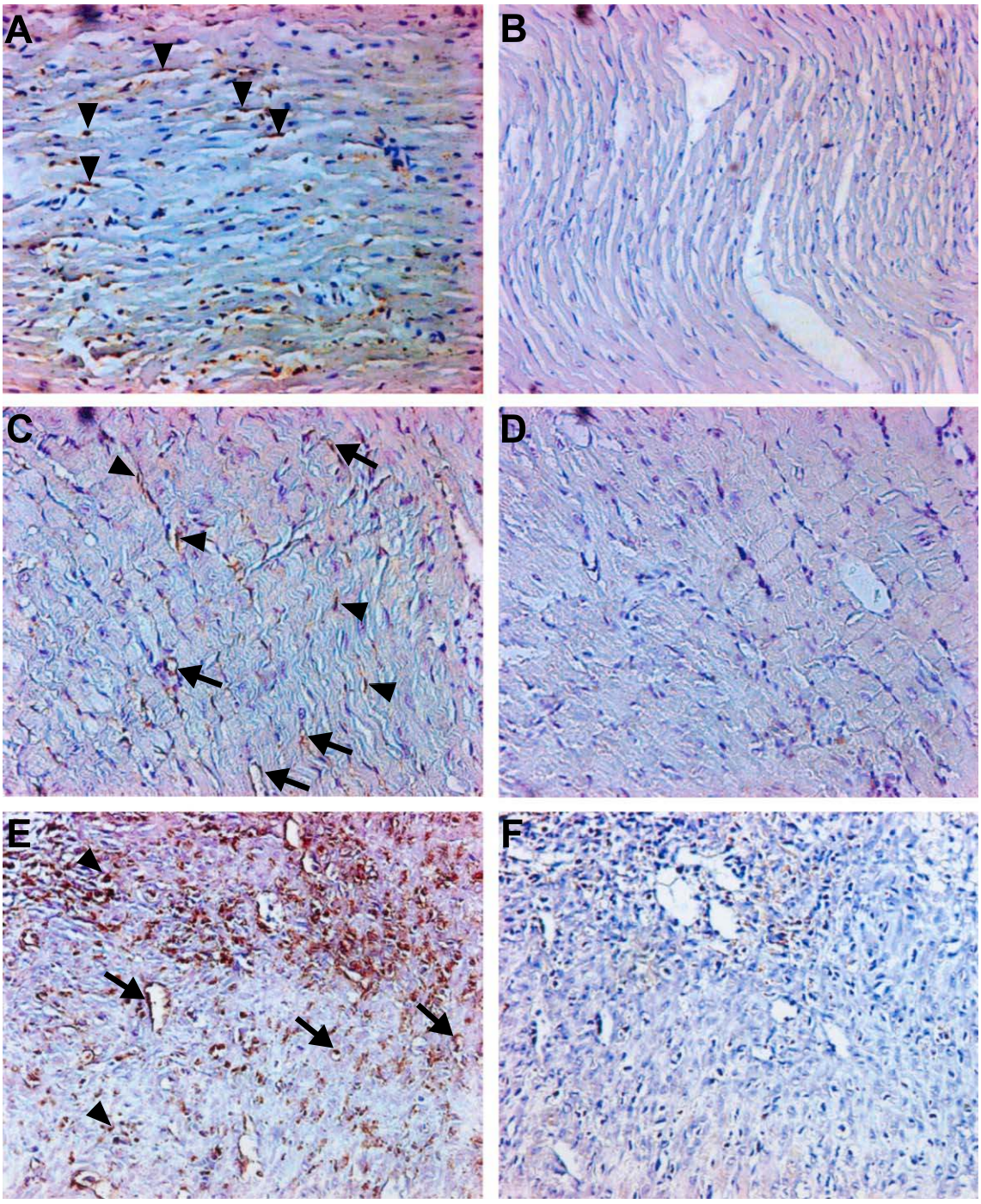

Fig. 4. Immunostaining of rat myocardial biglycan. The myocardial tissue sections from the non-ischemic LV region of a failing heart showing biglycan immunoreactivity in interstitial fibroblast-like cells (arrowheads) and endothelial cells (arrows) (A, C). Section from granulation and differentiating scar tissue of HF rat demonstrating biglycan expression in the fibroblast-like cells and in the microvascular endothelial cells (E). Tissue section from the LV of sham-operated rat showing weaker staining compared to HF rat (B). Myocardial tissue sections from non-ischemic LV region and from scar tissue of HF rat incubated with nonimmune chicken serum, demonstrating specificity of the purified biglycan antiserum (D and F, respectively). Magnification × 200.

3.3. In situ detection of biglycan mRNA

Fig. 3 demonstrates in situ hybridisation of a digoxigenin-labeled biglycan antisense riboprobe in sections of myocardial tissue 7 days after MI. The most intense staining of biglycan mRNA was observed in the granulation tissue and differentiating scar tissue in the transition zone between necrotic and viable myocardium (Fig. 3A). In this region, positive signals for biglycan mRNA were found in fibroblast-like cells and in vascular endothelial cells (Fig. 3C). However, biglycan mRNA expression was also seen in myocardial tissue distal to the infarcted zone, predominantly in fibroblast-like cells between the cardiomyocytes and in vascular endothelial cells (Fig. 3E). No signals were obtained with the digoxigenin-labeled sense riboprobe, confirming specificity of the biglycan antisense riboprobe at in situ hybridisation. (Fig. 3B,D,F).

3.4. Immunohistochemical analysis of the distribution of biglycan in the myocardium

Representative immunohistochemical staining of biglycan in myocardial tissue sections of rats 7 days after MI is shown in Fig. 4. In non-ischemic left ventricular tissue distal to the MI (Fig. 4A and C), robust immunoreactivity was detected in fibroblast-like cells and endothelial cells of interstitial tissue. The cardiomyocytes, on the other hand, displayed very faint immunostaining or in many instances hardly any detectable immunoreactivity at all. In the granulation tissue and differentiating scar tissue replacing necrotic myocardial tissue (Fig. 4E), intense immunoreactivity confined to fibroblast-like cells and endothelial cells were found. Immunostaining of the interstitial tissue in myocardial sections of MI rats was substantially stronger than that of sham rats (Fig. 4A and B), consistent with the Northern blot analyses demonstrating elevations of myocardial biglycan mRNA levels after MI. No immunostaining was seen in myocardial tissue sections incubated with nonimmune chicken serum, demonstrating specificity of the purified biglycan antibody (Fig. 4D and F).

3.5. Effects of AT_1 receptor antagonism on hemodynamic parameters and myocardial hypertrophy in HF

Male Wistar rats subjected to MI were randomised to treatment with losartan or vehicle as described in Methods. After completion of the 25 days intervention protocol, hemodynamic recordings revealed characteristic abnormalities of HF with decreased LVSP and increased LVEDP in the HF-vehicle group compared with sham rats (Table 3). The HF-vehicle rats also demonstrated significantly elevated lung weight-to-body weight ratios compared with sham-operated rats, indicating severe cardiac dysfunction with pulmonary congestion.

Table 3
Hemodynamic measurements in sham-operated and HF rats after 25 days treatment with losartan or vehicle

	Sham ($n=5$)	HF-vehicle ($n=5$)	HF-losartan ($n=6$)
HW/BW, mg/g	2.54 ± 0.04	3.40 ± 0.14*	3.00 ± 0.11*,†
LV/BW, mg/g	1.80 ± 0.02	2.02 ± 0.04*	1.82 ± 0.05†
RV/BW, mg/g	0.46 ± 0.015	0.72 ± 0.6*	0.56 ± 0.03*,†
Scar wt/BW, mg/g		0.55 ± 0.34	0.55 ± 0.31
Lung wt/BW, mg/g	3.76 ± 0.04	7.05 ± 0.92*	4.74 ± 0.41*,†
MAP, mm Hg	130 ± 5	112 ± 5*	100 ± 5*
LVSP, mm Hg	149 ± 7	125 ± 8*	115 ± 6*
LVEDP, mm Hg	2 ± 1	16 ± 3*	11 ± 2*
+dP/dt (mm Hg/s)	6463 ± 445	4447 ± 537*	4760 ± 108*

HW, heart weight; BW, body weight; MAP, mean arterial pressure; LVSP, LV systolic pressure; LVEDP, LV end-diastolic pressure; +dP/dt, peak rate of LV pressure increase.
Values are mean ± S.E.
* $P<0.05$ vs. sham-operated rats.
† $P<0.05$ vs. HF-vehicle rats.

However, as shown in Table 3, there were no statistical differences of MAP, LVSP, and LVEDP in the HF-losartan group compared with the HF-vehicle group, although the group means of the three hemodynamic parameters were all lower in the HF-losartan group compared with the HF-vehicle group. Losartan, on the other hand, significantly blunted the development of right ventricular hypertrophy. The left ventricular weight-to-body weight ratio was also significantly decreased in the HF-losartan group compared with the HF-vehicle group. Furthermore, the lung weight-to-body weight ratio was also substantially lower in the HF-losartan group compared with the HF-vehicle group (4.74 ± 0.41 vs. 7.05 ± 0.92 mg/g; $P<0.05$), indicating alleviation of pulmonary congestion. Thus, the data consistently indicate improved cardiac function after treatment with losartan.

3.6. Effects of AT_1 receptor antagonism on myocardial biglycan and TGF-β_1 mRNA expression in HF

Real-time quantitative RT-PCR demonstrated 2.5-fold increase of biglycan mRNA levels in the non-ischemic, viable LV of HF-vehicle rats 28 days after MI compared with sham-operated rats ($P<0.05$). AT_1 receptor antagonism prevented the induction of myocardial biglycan mRNA after MI. As shown in Fig. 5A, there were no significant differences of biglycan mRNA levels between the sham-operated group and the HF-losartan group. Similar induction of myocardial TGF-β_1 mRNA as well as its inhibition by losartan was observed in the HF-vehicle and HF-losartan groups, respectively (Fig. 5B). Both biglycan and TGF-β_1 mRNA levels are presented relative to GAPDH mRNA levels as the housekeeping gene (Fig. 5A and B). GAPDH mRNA levels did not display differences in any of the groups which would significantly impact on the reported regulation of biglycan and TGF-β_1 (mean C_T values of GAPDH mRNA ± S.E.M. were 24.70 ± 0.1659, 24.49 ± 01129, and 25.01 ± 0.3115 in the

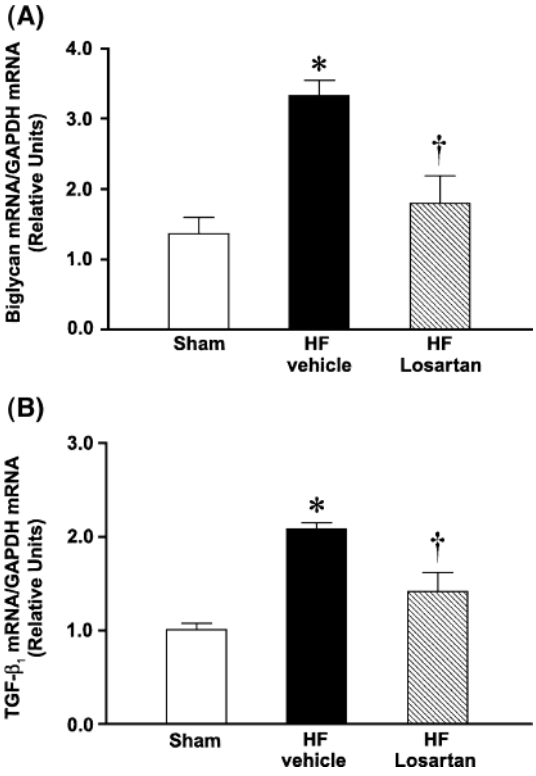

Fig. 5. Quantitative real-time RT-PCR analysis demonstrating the effects of 25 days of treatment with losartan on biglycan mRNA (A), and on TGF-β_1 mRNA levels in the non-ischemic LV of HF rats (B). Data are presented as ratios of biglycan or TGF-β mRNA levels relative to levels of GAPDH mRNA, mean ± S.E. (Sham group, $n=5$; HF-vehicle group, $n=5$; HF-losartan group, $n=6$). * $P<0.05$ vs. sham-operated group; † $P<0.05$ vs. HF-vehicle group.

sham-operated group, HF-vehicle group and HF-losartan group, respectively; $P>0.2$).

3.7. Quantification of biglycan mRNA levels in isolated cardiac fibroblasts

To provide evidence of regulation of biglycan mRNA levels in rat cardiac fibroblasts from failing hearts, we isolated cardiac fibroblasts of hearts from sham-operated and HF rats. mRNA expression was analysed by real-time quantitative RT-PCR. As shown in Fig. 7A, biglycan mRNA levels were significantly elevated in cardiac fibroblasts from HF rats as compared with those from sham-operated rats (55 ± 6.287 vs. 6.5 ± 0.8174; $P<0.05$). Thus, the data are consistent with the immunohistochemical analysis and in situ hybridisation of myocardial tissue samples, demonstrating robust induction of biglycan expression in myocardial fibroblasts of HF rats.

3.8. Effects of Ang II on expression of biglycan and TGF-β_1 mRNA in cardiac fibroblasts

Recombinant adenovirus was employed to overexpress the angiotensin AT_{1A} receptor in isolated cardiac fibroblasts. Expression of adenoviral transgenes including the prokaryotic LacZ cDNA (employed as control) is shown in Fig. 6. As shown in Fig. 7B, Ang II (100 nmol/l; 24 h stimulation) induced expression of biglycan mRNA in cardiac fibroblasts infected with recombinant adenovirus encoding the AT_{1A} receptor cDNA. Losartan (10 μmol/l) prevented the stimula-

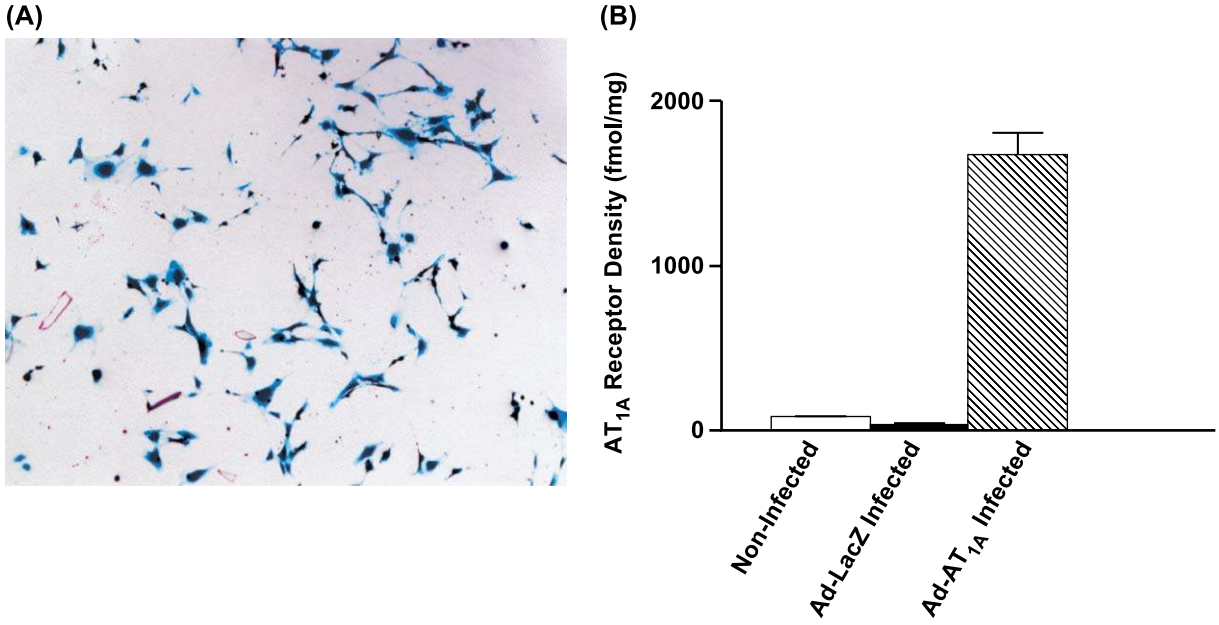

Fig. 6. Expression of recombinant adenoviral transgenes in adult rat cardiac fibroblasts. Fibroblasts were infected at MOI of 100 for 24 h. As assessed by X-gal staining, Ad-LacZ was shown to infect virtually all fibroblasts (A). Radioligand binding assays of [^{125}I]-Ang II performed on crude membrane particles from non-infected, and Ad-LacZ- and Ad-AT_{1A}-infected cardiac fibroblasts. The data represent the ± S.E.M. of three independent experiments, each performed in triplicate (B).

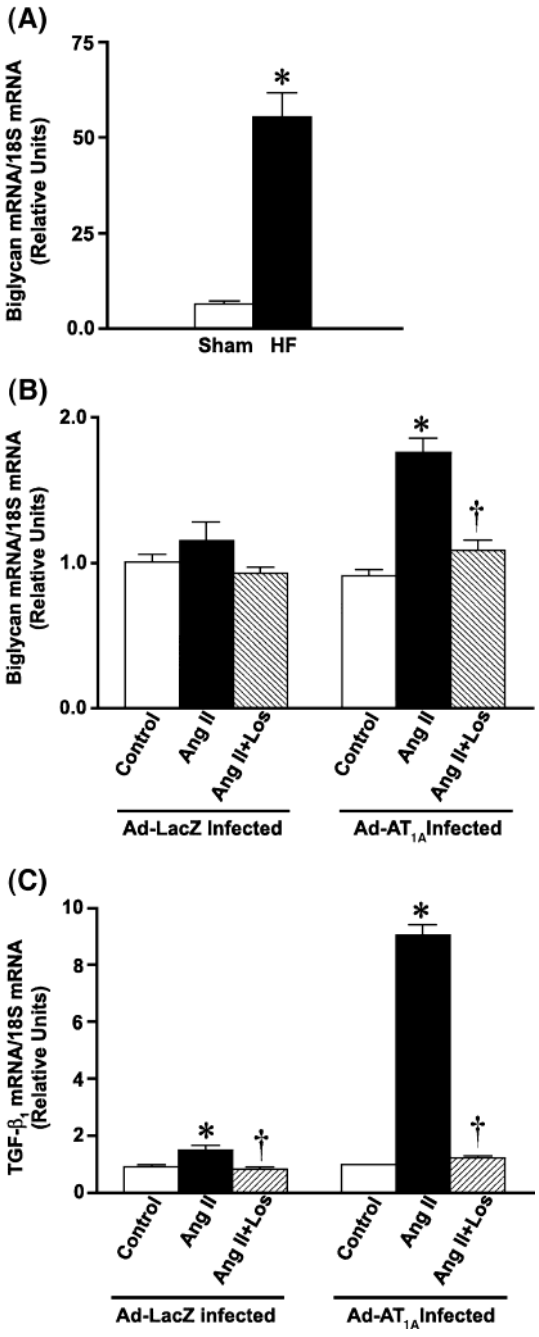

Fig. 7. Quantitative real-time RT-PCR analysis demonstrating differential expression of biglycan mRNA in rat cardiac fibroblasts from sham-operated rats and HF rats (A). Quantitative real-time RT-PCR analysis of biglycan mRNA levels in cardiac fibroblasts infected with Ad-LacZ (MOI 100) or Ad-AT_{1A} and (MOI 100) incubated in the absence or presence of Ang II (100 nmol/l; 24 h) or Ang II and Losartan (100 nmol/l and 10 μmol/l, respectively; 24 h) (B). Quantitative real-time RT-PCR analysis of TGF-β_1 mRNA levels in cardiac fibroblasts incubated in the absence or presence of Ang II (100 nmol/l; 24 h) or Ang II and Losartan (100 nmol/l and 10 μmol/l, respectively; 24 h) (C). Data are presented as ratios of biglycan mRNA levels relative to levels of 18S RNA. Mean ± S.E., $^*P<0.05$ vs. control group; $^\dagger P<0.05$ vs. Ang II group.

tory effect of Ang II on the mRNA levels of biglycan implicating an AT_1 receptor-dependent mechanism. On the other hand, Ang II did not cause significant elevations of biglycan mRNA levels in Ad-LacZ-infected cardiac fibroblasts, indicating that endogenous AT_1 receptors were too low to enable significant stimulation of biglycan mRNA expression levels. However, as shown in Fig. 7C, Ang II (100 nmol/l; 24 h stimulation) induced expression of TGF-β_1 mRNA in Ad-LacZ-infected cardiac fibroblasts, and even more robust TGF-β_1 mRNA expression was observed in Ad-AT_{1A}-infected cells. Losartan significantly inhibited the Ang II-stimulated TGF-β_1 mRNA levels.

4. Discussion

In the present study, we report novel evidence implicating the multifunctional proteoglycan, biglycan in remodelling of myocardial tissue of the failing heart. The study demonstrates that myocardial expression of biglycan is substantially induced in the non-ischemic tissue of both the left and the right ventricles of rats with HF after experimentally induced MI. Biglycan mRNA levels in non-ischemic myocardial tissue were increased already 2 days after MI. Although peak levels of expression were observed at day 7 post-MI, biglycan mRNA levels were substantially elevated at 42 days after induction of MI, a time point at which the scar tissue replacing the necrotic tissue was fully differentiated and healed. Thus, our data demonstrate that the induction of myocardial biglycan transcends from early to late phase of post-infarction remodelling, supporting the notion that biglycan is involved in the pathophysiology of HF. In this respect, we also demonstrate that induction of myocardial biglycan mRNA is related to neurohormonal activation associated with HF. As shown, induction of myocardial biglycan mRNA in rats with HF could be prevented by treatment of the rats with an AT_1 receptor antagonist, indicating a role of Ang II in regulation of biglycan.

The in situ hybridisation reported in this study demonstrates robust expression of biglycan mRNA in both fibroblast-like cells and endothelial cells of non-ischemic myocardial tissue from rats with HF. Such global cardiac induction of biglycan mRNA has not previously been recognized. In a previous study of rats subjected to ligation of the left coronary artery, expression of biglycan mRNA in fibroblasts in the granulation tissue replacing ischemic myocardial tissue was reported [10]. These findings are confirmed in the present study indicating that biglycan may contribute to healing of the scar after MI. However, our data also call for a role of biglycan in remodelling of non-ischemic myocardial tissue.

In the normal heart, collagen fibrils form molecular tethers that support and align cardiac myocytes and blood vessels in order to maintain myocardial tissue integrity as well as ventricular geometry. The amount of myocardial collagen depends on the balance between synthesis and degradation of

collagen [15,29]. HF is associated with increased deposition of extracellular collagen due to increased synthesis [16]. However, the stability and functionality of collagen do not only depend on the total amount of collagen, but also on the organisation of fibrils and on the degree of covalent cross-linkages between fibrils [15]. Biglycan has been shown to bind collagen [4], and current evidence supports the concept that biglycan is involved in proper organisation of collagen fibril networks [17]. Proper three-dimensional organisation of collagen fibril networks may also protect from metalloproteinase-mediated degradation and thereby promote accumulation of collagen [18]. However, biglycan may subserve additional functions relevant to the pathophysiology of myocardial remodelling. It has previously been reported that biglycan binds TGF-β with fairly high affinity [6]. Heterodimerisation with TGF-β may affect both the availability, i.e. the local concentration, and the activity of TGF-β, an important mediator of fibroblast proliferation and synthesis of extracellular matrix components, particularly collagen and fibronectin [19]. Indeed, a substantial body of evidence points to an important role of TGF-β in myocardial remodelling and fibrosis in HF [20]. Thus, induction of myocardial biglycan in HF may shift the equilibrium of the interaction between biglycan and TGF-β and enhance TGF-β activity in the myocardial tissue.

Neurohormones, autocrine/paracrine factors, as well as increased ventricular wall stress may all be envisaged as potential inducers of myocardial biglycan expression in HF. In the present study we demonstrate AT_1 receptor antagonist losartan prevented the induction of myocardial biglycan mRNA expression in rats with ischemic HF. Thus, our data indicate that the increased circulating levels of Ang II in HF may act as an important stimulator of myocardial biglycan mRNA expression. Similar AT_1 receptor-dependent stimulation of biglycan mRNA has been reported in the renal tissue from spontaneously hypertensive rats [21]. Previous studies with angiotensin converting enzyme inhibitors or AT_1 receptor antagonists in experimental models of HF have shown that these interventions prevent development of interstitial fibrosis of myocardial tissue [22,23]. Furthermore, the beneficial effects of Ang II antagonism on myocardial remodelling, ventricular compliance, and diastolic function can be attributed to large extents to the effects of the drugs on myocardial collagen content [24,25]. Ang II has been reported to stimulate biglycan mRNA expression in vascular smooth muscle cell lines [26,27]. However, as reported in the present study, Ang II did not cause significant elevations of biglycan mRNA levels of primary cultures of cardiac fibroblasts. On the other hand, in cultured cardiac fibroblasts overexpressing the AT_1 receptor, Ang II stimulated marked elevations of biglycan mRNA, supporting the notion that endogenous levels of AT_1 receptors in cultured cardiac fibroblasts were not sufficient to enable induction of biglycan mRNA. It is well documented that cardiac fibroblasts dedifferentiate upon propagation in culture and that AT_1 receptor densities decline drastically. Analysis of AT_1 receptor densities in the cardiac fibroblasts isolated in the present study showed that AT_1 receptor levels declined from 120 fmol/mg membrane protein to approximately 30 fmol/mg membrane protein upon the first two passages (data not shown). Thus, dedifferentiation of isolated fibroblasts upon culture is a plausible explanation of the lack of AT_1 receptor-dependent stimulation of biglycan mRNA levels. Ang II has been shown to simulate TGF-β_1 mRNA expression in rat mesangial cells [28]. Furthermore, TGF-β has been reported to stimulate the synthesis and secretion of proteoglycans in primary cultures of myocardial fibroblasts [29]. However, our data do not support the hypothesis that TGF-β_1 acts as a mediator of Ang II-stimulated induction of biglycan mRNA. Thus, the signalling pathway of Ang II-stimulated biglycan mRNA does not appear to involve TGF-β_1 in cardiac fibroblasts.

The increased load on the heart during HF with increased wall stress may constitute another mechanism of induction of myocardial biglycan mRNA. Indeed, in vitro experiments on isolated fibroblasts demonstrate that increased stretch stimulates synthesis and release of biglycan [30]. In the present study, losartan did not cause significant reductions of LVEDP, LVSP, and MAP. However, based on the small number of rats in each group and the fact that LVEDP, LVSP, and MAP all demonstrated a declining trend, one cannot exclude the possibility that, at least partially, the effects of losartan on myocardial biglycan mRNA expression could be secondary to reductions of both preload and afterload.

In conclusion, we have demonstrated global cardiac induction of biglycan in experimentally induced HF in rats. In situ hybridisation and analysis of primary isolates of cardiac fibroblasts demonstrated that myocardial induction of biglycan mRNA was confined to fibroblasts. Furthermore, we provide evidence of Ang II-stimulated induction of biglycan mRNA in cardiac fibroblasts. In this respect, the present study demonstrates that induction of myocardial biglycan in rats with HF can be prevented by AT_1 receptor antagonism, an intervention well documented to halt cardiac dysfunction and pathologic remodelling in HF. Future investigations will emphasize on elucidation of the role of myocardial biglycan in myocardial remodelling and progression of HF.

Acknowledgements

This study was supported by grants from the National Research Council and the Norwegian Council for Cardiovascular Research.

References

[1] Colucci WS. Molecular and cellular mechanisms of myocardial failure. Am J Cardiol 1997;80:15L–25L.
[2] Kjellen L, Lindahl U. Proteoglycans: structures and interactions [pub-

lished erratum appears in Annu Rev Biochem 1992;61:following viii]. Annu Rev Biochem 1991;60:443–75.
[3] Ruoslahti E, Yamaguchi Y. Proteoglycans as modulators of growth factor activities. Cell 1991;64:867–9.
[4] Schonherr E, Witsch-Prehm P, Harrach B, Robenek H, Rauterberg J, Kresse H. Interaction of biglycan with type I collagen. J Biol Chem 1995;270:2776–83.
[5] Couchman JR, Austria MR, Woods A. Fibronectin–cell interactions. J Invest Dermatol 1990;94:7S–14S.
[6] Hildebrand A, Romaris M, Rasmussen LM, et al. Interaction of the small interstitial proteoglycans biglycan, decorin and fibromodulin with transforming growth factor beta. Biochem J 1994;302: 527–34.
[7] Bianco P, Fisher LW, Young MF, Termine JD, Robey PG. Expression and localization of the two small proteoglycans biglycan and decorin in developing human skeletal and non-skeletal tissues. J Histochem Cytochem 1990;38:1549–63.
[8] Fisher LW, Heegaard AM, Vetter U, et al. Human biglycan gene. Putative promoter, intron–exon junctions, and chromosomal localization. J Biol Chem 1991;266:14371–7.
[9] Ungefroren H, Krull NB. Transcriptional regulation of the human biglycan gene. J Biol Chem 1996;271:15787–95.
[10] Yamamoto K, Kusachi S, Ninomiya Y, et al. Increase in the expression of biglycan mRNA expression co-localized closely with that of type I collagen mRNA in the infarct zone after experimentally-induced myocardial infarction in rats. J Mol Cell Cardiol 1998;30:1749–56.
[11] Oie E, Vinge LE, Tonnessen T, et al. Transient, isopeptide-specific induction of myocardial endothelin-1 mRNA in congestive heart failure in rats. Am J Physiol 1997;273:H1727–36.
[12] Oie E, Bjonerheim R, Grogaard HK, Kongshaug H, Smiseth OA, Attramadal H. ET-receptor antagonism, myocardial gene expression, and ventricular remodeling during CHF in rats. Am J Physiol 1998;275: H868–77.
[13] Sasamura H, Hein L, Krieger JE, Pratt RE, Kobilka BK, Dzau VJ. Cloning, characterization, and expression of two angiotensin receptor (AT-1) isoforms from the mouse genome. Biochem Biophys Res Commun 1992;185:253–9.
[14] Vinge LE, Oie E, Andersson Y, Grogaard HK, Andersen G, Attramadal H. Myocardial distribution and regulation of GRK and beta-arrestin isoforms in congestive heart failure in rats. Am J Physiol, Heart Circ Physiol 2001;281:H2490–9.
[15] Ju H, Dixon IM. Extracellular matrix and cardiovascular diseases. Can J Cardiol 1996;12:1259–67.
[16] Peters TH, Sharma HS, Yilmaz E, Bogers AJ. Quantitative analysis of collagens and fibronectin expression in human right ventricular hypertrophy. Ann N Y Acad Sci 1999;874:278–85.
[17] Wiberg C, Heinegard D, Wenglen C, Timpl R, Morgelin MM. Biglycan organizes collagen VI into hexagonal-like networks resembling tissue structures. J Biol Chem 2002.
[18] Hunzelmann N, Anders S, Sollberg S, Schonherr E, Krieg T. Coordinate induction of collagen type I and biglycan expression in keloids. Br J Dermatol 1996;135:394–9.
[19] de Andrade CR, Cotrin P, Graner E, Almeida OP, Sauk JJ, Coletta RD. Transforming growth factor-beta1 autocrine stimulation regulates fibroblast proliferation in hereditary gingival fibromatosis. J Periodontol 2001;72:1726–33.
[20] Lijnen PJ, Petrov VV, Fagard RH. Induction of cardiac fibrosis by transforming growth factor-beta(1). Mol Genet Metab 2000;71: 418–35.
[21] Sasamura H, Shimizu-Hirota R, Nakaya H, Saruta T. Effects of AT1 receptor antagonist on proteoglycan gene expression in hypertensive rats. Hypertens Res 2001;24:165–72.
[22] Silvestre JS, Heymes C, Oubenaissa A, et al. Activation of cardiac aldosterone production in rat myocardial infarction: effect of angiotensin II receptor blockade and role in cardiac fibrosis. Circulation 1999;99:2694–701.
[23] Varo N, Etayo JC, Zalba G, et al. Losartan inhibits the post-transcriptional synthesis of collagen type I and reverses left ventricular fibrosis in spontaneously hypertensive rats. J Hypertens 1999;17:107–14.
[24] Zhu YZ, Zhu YC, Li J, et al. Effects of losartan on haemodynamic parameters and angiotensin receptor mRNA levels in rat heart after myocardial infarction. J Renin-Angiotensin-Aldosterone Syst 2000;1: 257–62.
[25] Kim S, Sada T, Mizuno M, et al. Effects of angiotensin AT1 receptor antagonist on volume overload-induced cardiac gene expression in rats. Hypertens Res 1997;20:133–42.
[26] Figueroa JE, Vijayagopal P. Angiotensin II stimulates synthesis of vascular smooth muscle cell proteoglycans with enhanced low density lipoprotein binding properties. Atherosclerosis 2002;162:261–8.
[27] Shimizu-Hirota R, Sasamura H, Mifune M, et al. Regulation of vascular proteoglycan synthesis by angiotensin II type 1 and type 2 receptors. J Am Soc Nephrol 2001;12:2609–15.
[28] Kagami S, Border WA, Miller DE, Noble NA. Angiotensin II stimulates extracellular matrix protein synthesis through induction of transforming growth factor-beta expression in rat glomerular mesangial cells. J Clin Invest 1994;93:2431–7.
[29] Heimer R, Bashey RI, Kyle J, Jimenez SA. TGF-beta modulates the synthesis of proteoglycans by myocardial fibroblasts in culture. J Mol Cell Cardiol 1995;27:2191–8.
[30] Xu J, Liu M, Liu J, Caniggia I, Post M. Mechanical strain induces constitutive and regulated secretion of glycosaminoglycans and proteoglycans in fetal lung cells. J Cell Sci 1996;109(Pt. 6):1605–13.